Departament de Medicina / Universitat Autónoma de Barcelona

TREBALL DE RESERCA JUNY 2010

GDAP1-related autosomal dominant Charcot-Marie-Tooth disease: phenotypical and MRI features

Autor: Rafael Sivera Mascaró

Director: Dr Jose Álvarez Sabin

Co-director: Dra. Maria Teresa Sevilla Mantecón

INDEX:

SUMMARY

Background: Mutations in the *ganglioside-induced-differentiation-associated-protein 1* (*GDAP1*) gene have been reported in Charcot Marie Tooth (CMT) patients, most of which have a recessive form of inheritance. So far, only a few families with autosomal dominant (AD) inheritance have been reported and the phenotype is not fully characterized.

Methods: A systematic search for *GDAP1* mutations was performed in a large clinically well characterized CMT series in which mutations in the most prevalent genes involved in CMT had been excluded. All patients were clinically evaluated, and neurophysiological studies, muscle magnetic resonance imaging (MRI), and sural nerve biopsy were performed when possible.

Results: We identified 4 unrelated families (17 patients) with the same causative point mutation in the *GDAP1* gene (p.R120W) which was inherited as an AD trait.

The clinical picture included a mild-moderate phenotype with onset around adolescence, but a great clinical heterogeneity, ranging from elderly asymptomatic patients to others in which independent deambulation is difficult. Consistently, ankle dorsiflexion and plantar flexion were impaired to a similar degree. Nerve conduction studies were compatible with an axonal neuropathy. MRI studies demonstrated selective involvement of intrinsic foot muscles in all patients and a uniform pattern of fatty infiltration in the calf, with distal and superficial posterior predominance. Pathologic data was similar to recessive GDAP1 mutations.

Conclusions: This work extends the understanding of the pathogenesis of *GDAP1* associated CMT and suggests that mutations in this gene should also be considered in patients with CMT2 phenotype independently of the inheritance pattern and severity of the disease.

INTRODUCTION

Charcot- Marie-Tooth disease (CMT) is a genetically heterogeneous group of inherited motor and sensory neuropathies. Molecular studies have shown extensive genetic heterogeneity in CMT neuropathies with an evergrowing list of causative mutations and loci.[1] Mutations in the *ganglioside-induced-differentiation-associated protein 1* (*GDAP1*) gene 8q21 have been reported in CMT patients with demyelinating (CMT4A) [2] and axonal forms (CMT2K and ARCMT2K) of the disease.[3] Inheritance in most causative *GDAP1* mutations is autosomal recessive, [4-6] characterized by a severe phenotype with early disease onset and rapid progression to important disability in the second or third decade. In recent reports certain mutations have been shown to segregate as an autosomal dominant trait with a later disease onset and a mild phenotype[4,7,8] being the p.R120W missense mutation the most prevalent one.[4,9]

The utility of muscle MRI in CMT is still to be defined, being a potentially useful method for identifying areas of muscle atrophy and fatty infiltration that occur secondary to denervation. The presence of high signal intensity within skeletal muscle on T2-weighted images, and short tau inversion recovery (STIR) in the correct clinical context are suggestive of denervated muscles.[10,11] The main objective is to describe a characteristic pattern of muscle involvement that can be correlated with the different phenotypes and/or genotypes.

To achieve a complete phenotypic characterization of patients with autosomal dominant p.R120W mutation in the *GDAP1* gene we provide extensive clinical and electrophysiological data, as well as muscle magnetic resonance images from a series of 17 CMT patients belong to 4 unrelated families.

PATIENTS AND METHODS

Subjects

A systematic search for *GDAP1* mutations was performed in a large clinically well characterized CMT series in which mutations in the most prevalent genes involved in CMT (*PMP22*, *MPZ* and *GJB1)*, had been excluded independently of the observed phenotype. In CMT2 patients mutations in the *MFN2*, *NEFL*, *MPZ*, *GJB1* and *LITAF* genes were also discarded. We identified 17 patients from 4 unrelated families with *GDAP1* mutations in which disease appeared to be inherited as an autosomal dominant trait. All protocols performed in this study complied with the ethics guidelines of the institutions involved. The pedigrees are displayed in figure 1.

Mutation analysis

Blood samples were drawn from the patients and relatives after informed consent and in accordance with the Helsinki declaration. Genomic DNA was obtained by standard methods from peripheral white blood cells. Mutation analysis of the *GDAP1* gene was performed by amplification of the 6 exons and their intronic flanking sequences using primers previously described.[3] The PCR products were analyzed by DHPLC (*Denaturing High Liquid Chromatography*, Transgenomic WAVE® System) and the anomalous patterns were investigated by automated sequencing (ABI Prism 3130xl, Applied Biosystems). When possible, segregation analyses were performed.

Clinical assessments

All probands and individuals at-risk were examined except patients B-II3 and B-III2. The clinical assessment included strength, muscle atrophy, sensory loss, reflexes, foot deformities as well as a general and neurologic examination. Muscle strength was

graded using the standard Medical Research Council (MRC) scale. CMT neuropathy score (CMTNS) was applied to determine neurological impairment: mild (CMTNS<10 points), moderate (CMTNS 11–20) and severe (CMTNS 21–36).[12] The functional disability scale (FDS) [13] was used to measure the disability caused by the disease. The data of family B had been partially reported previously.[4]

Electrophysiological studies

Electrophysiological studies were performed in 14 of the patients. Nerve conduction studies (NCS) were tested with surface electrodes. Amplitudes of compound muscle action potentials (CMAPs), distal latency (DL) and conduction velocity from median, ulnar, peroneal, tibial and axillary nerves were recorded using conventional methods. Recordings of sensory nerve action potentials (SNAPs) from median and ulnar nerves were performed orthodromically while sural nerve was tested antidromically. Concentric needle electromyography was performed in the proximal and distal muscles of the upper and lower limbs.

Magnetic resonance imaging

MRI was performed on the feet and distal legs of 8 patients in a supine position using a 1.5 T MR platform (Siemens Avanto, Erlangen, Germany). The following protocol was used in all patients: axial and coronal T1-weighted TSE (turbo spin echo), STIR, and T1 fat-saturation images before and after Gadolinum-DTPA (Magnevist, Schering, Germany) administration were obtained of both legs and feet. Only one imaging plane was acquired in each region after contrast administration.

The four classic anatomical compartments were used to evaluate calf muscles: anterior compartment (tibialis anterior, extensor hallucis longus, and extensor digitorum

longus), lateral compartment (peronei longus and brevis), superficial posterior compartment (soleus and gastrocnemius), and deep posterior compartment (tibialis posterior, flexor digitorum longus and flexor hallucis longus). In axial MR images of lower limbs, fatty infiltration was graded from 0 to 4 as follows: 0, no fat signal in muscle; 1, some fatty streaks; 2, fat occupying a minor part of muscle; 3, similar amount of fat and muscle tissue; 4, fat occupying the greater part of muscle.[13]

Nerve biopsies

Sural nerve biopsy was performed in two cases (patients A-II1 and C-II2) when they were 47 and 31 years old respectively, and compared to a 27 year-old multiorgan donor without neuropathic or systemic disease history. Semi-thin sections stained with toluidine blue were prepared for evaluation under a light microscope following the same protocol as described previously.[6] Morphometry of myelinated fibres was performed on high-resolution micrographic images obtained with a Polaroid DMC digital camera and analyzed by means of Scion image analyst software (http://www.scioncorp.com). Ultra-thin cut samples were contrasted with uranyl acetate and lead citrate for ultrastructural study.[6]

RESULTS

Mutation analysis

17 patients from four unrelated families carrying the *GDAP1* p.R120W mutation in a heterozygous state were identified. No other pathogenic mutations were identified in other exons or in their flanking intron regions. Autosomal dominant inheritance was confirmed by co-segregation of the *GDAP1* p.R120W mutation with disease in these four families.

Clinical findings

The clinical characteristics of 15 patients from the four families with the p.R120W missense mutation in the *GDAP1* gene are summarized in table 1.

The age in which patients experienced the first symptom ranged between 9 and 65 years (median 17 years), with disease duration between 5 and 48 years. There was no delay in the acquisition of motor milestones. Four patients (A-II2, A-II3, B-III1 and C-I2) aged 20, 38, 33 and 72 did not complain of any symptom but clinical examination revealed minor signs. Patient A-II2 had mild weakness in toe extension, hyporreflexia and hypoesthesia in lower limbs, patient A-II3 absent ankle reflexes and distal hypoesthesia, patient B-III1 pes cavus, and patient C-I2 absent knee and ankle jerks.

The disease started in the distal lower limbs. Only two patients had mild proximal involvement in the lower limbs (A-I1 and D-II1), being quite disabling in one case. All symptomatic cases presented weakness in ankle plantar flexion (EHL) and toe extension. Weakness in ankle dorsiflexors was present to the same degree as plantar flexors in most symptomatic patients, being the impairment of heel and toe walk quite analogous. Distal upper limb weakness appeared later in the course of the disease and

involved the intrinsic hand muscles predominately. At the time of the examination, 12 patients had motor deficits in distal lower limbs, 7 patients in both the distal lower and upper limbs. In one patient (C-II2), the distribution of muscle atrophy and weakness in the lower limbs was asymmetric. Proximal muscle strength was abnormal in lower limbs in 2 patients. All patients except two had preserved reflexes in the upper limbs, but hypo/arreflexia in lower limbs and different degrees of lower limb distal atrophy. Foot deformities, including pes cavus and Achilles tendon shortening were also very common. Sensory loss proportional to the motor deficit was present in all symptomatic patients, especially pinprick and vibration in distal lower limbs.

The CMTNS scores in the series reflected the wide phenotypic spectrum, ranging from 0-25. There were only two patients that were catalogued in the CMTNS severe category, both of which had a long disease evolution. Nine patients (60%) were in the mild category and 4 in the moderate. All patients to date have a functional disability scale equal or less than 4 except two patients, patient A-I1 who is mostly wheelchair bound, and patient D-II1 who needs a cane or crutches to walk. Disease progression was slow in the majority of cases but two patients (A-I1 and B-I4) had onset after 40, but developed a relevant functional impairment.

Electrophysiological studies

Table 2 summarizes the nerve conduction and electromyography studies performed. Motor nerve conduction velocities, distal latencies and f waves were normal in all tested nerves (median MNCV > 54 m/sec in all patients). Ulnar and median CMAP were reduced only in two individuals, but peroneal CMAP was reduced in most affected individuals. Sensory nerve conduction was altered in all patients, with a reduction of SNAP, but normal conduction velocities and distal latencies in the tested

nerves with SNAP > 0.5 μv. In all patients, even if asymptomatic, needle electromyography revealed MUAPs (motor unit action potentials) increased in amplitude, duration and polyphasic incidence. Positive sharp waves and fibrillation potentials were not present.

MRI studies

All patients had detectable abnormalities in the MRI consisting in fatty infiltration and/or muscle edema (table 2).

Intrinsic musculature of both feet showed consistent and bilateral fatty infiltration of the foot muscles in all patients, even in asymptomatic ones (figure 2A). The changes were present in all intrinsic foot muscles and were more pronounced in severely affected patients. All patients had evidence of varying degrees of fatty substitution in the muscles of the calf in concordance with the severity of the phenotype. In any case there was a common pattern: a predominance of fatty substitution distally and in the posterior compartment over the anterolateral one.

Mild cases showed distinct abnormalities in the distal muscles of the calf; high signal intensity on T1-weighted and STIR images, corresponding with fatty substitution and muscle edema respectively. The muscle affected first and to a greater degree was the gastrocnemius and to a slightly lesser degree the soleus (figure 2B), being the rest of the muscles in the calf completely preserved in most mild cases.

In more severe cases the fatty substitution involved all muscle compartments of the calf and muscle edema was no longer present. The posterior compartment was always affected to a greater degree than the anterolateral one with a mean grade of 3.1 vs. 1.5 ($p<0.05$) (figure 2C). MRI of the thigh was performed in only 2 patients (A-II1 and D-II1) with a moderate-severe phenotype, existing fatty substitution distally in all the

muscles.

Pathologic findings

The two sural nerves biopsies performed revealed similar pathological findings. Semi-thin sections showed a pronounced depletion of myelinated fibres in both nerves (fibre density was 3202/mm^2 in patient A-II1, 5863/mm^2 in patient C-II2, and 9095/mm^2 in the control subject). The histograms of myelinated fibre size were 'shifted to the left' showing a marked reduction of large-diameter fibres especially in patient A-II1 (the proportion of fibre size>6 μm was 12,3 % in A-II1, 31,5% in C-II2 and 41,7% in control) (figure 3A). Morphometric data also revealed a decrease in myelin thickness in proportion to the axonal diameter with a high proportion of fibres with a g-ratio > 0.7 (18.2% in A-II1, 20.9% in C-II2 and 5% in control).

Rather frequent regenerative clusters and occasional onion bulb formations were also present (figure 3B). In detailed electron-microscope views, onion bulbs were made up of concentric layers of Schwann cell processes adopting a crescent shape that included some amyelinic fibers. These formations enclosed a center composed of a regenerative cluster or less frequently a hypomyelinated or normally myelinated fibre (fig 3C). These formations had a limited number of folds (pseudo-bulbs) not reaching the size observed in CMT1A. The regenerative clusters were composed of a group of small myelinated fibres, a large bundle of unmyelinated axons or a combination of the two (figure 3F).

On high magnification, myelin compaction always appeared normal. However, axons often presented degenerative features consisting on axolemma retraction with partial or total detachment (fig3D), aggregation of normal and abnormal mitochondrial mixed with empty vacuoles, and cytoskeleton dissolution with early disappearance of

microtubules (figure 3E). Degeneration involved both myelinated and unmyelinated axons with preference for those included in regenerative clusters (figure 3F).

DISCUSSION

Autosomal dominant *GDAP1* mutations are exceedingly rare in most published CMT series. Here we present the clinical records belonging to 17 carriers of the *GDAP1* p.R120W mutation from four families.

The clinical picture comprehends a mild-moderate phenotype with great clinical heterogeneity. Disease onset varies, and duration is not clearly related to phenotypic severity. The identification of four asymptomatic mutation carriers, one of whom was already age 72, suggests that the p.R120W mutation may have incomplete penetrance. Weakness is first manifested distally in the lower limbs with the peculiarity that ankle dorsi and plantar flexors were impaired in similar degrees, as were tiptoe and heel walking. This picture contrasts with the typical CMT1A patients, which usually begin with foot drop due to weakness of ankle dorsiflexors,[13] being more similar to patients with late onset *MFN2* (*mitofusin 2*) mutations (CMT2A) in which there may exist a predominance of ankle plantar flexion weakness and greater difficulty in toe than in heel walking.[14]

Comparing the distribution of motor weakness in autosomal dominant patients with patients carrying recessive *GDAP1* mutations is quite a difficult task, due to the severity and the rapid disease progression in the latter. In our series with recessive *GDAP1* mutations,[6,15] characterization of the distal distribution weakness has been possible only in 2 who had a slightly more indolent course. In these patients the motor weakness in ankle plantar and dorsiflexion was similar, as was the impairment of toe and heel walking, findings quite analogous to the dominant forms. None of the dominant patients had stridor or voice hoarseness, a common characteristic in recessive forms.[5, 6,15-18] Proximal muscles were involved late in the course of the disease in some patients, causing impairment of independent ambulation.

Nerve conduction studies in our series revealed motor velocities in the axonal range with mildly reduced or normal CMAP amplitudes. Needle electromyography exposed giant motor units even in asymptomatic patients. This finding was very consistent in our series and has been already described in another family with the p.C240Y dominantly inherited mutation in *GDAP1*.[8] The physiopathology of this remains unclear, but is consistent with the slowly progressive nature of disease permitting significant collateral sprouting and hence motor unit remodelling.

The pathologic study of the two sural nerve biopsies performed was quite homogeneous and very similar to those described in the recessive *GDAP1* mutations, although the fiber loss was clearly more prominent in recessive forms.[6]. The main abnormalities were, loss of myelinated fibres and axonal degenerative features. The presence of regenerative clusters was prominent, and may represent a true reparative process of sprouting after axonal damage, or a developmental abnormality. Whatever the origin, these sprouted fibres could account for the high proportion of hypomyelinated fibres in the morphometric data. The presence of the small onion bulb formations is not yet explained, but probably do not correspond to a purely demyelinating phenomenon, as the conduction velocities are clearly in the axonal range and the same findings have been reported in other axonal neuropathies like *MFN2*mutations.[19]

In our series, the pattern of muscle abnormalities in MRI was quite homogeneous and concordant with disease severity. The main abnormalities described in these patients are fatty substitution of affected muscles, atrophy and occasionally edema (in subacute muscle denervation). The first muscles affected were the intrinsic foot and distal calf muscles, with a clear predominance of the posterior over the anterolateral compartment. This pattern is the same as that reported in CMT2A,[14] and quite

different from CMT1A[20] where there is a predominance of fatty substitution in the anterolateral compartment of the calf.

Most of *GDAP1* mutations co-segregate with CMT in an autosomal recessive manner,[2-6, 15-18] whereas autosomal dominant *GDAP1* mutations are rare. Mutations causative of an axonal CMT neuropathy with both dominant and recessive patterns of inheritance have been reported in three other genes: *NEFL*,[21-22] *HSP2*[23] and *MFN2*.[24-25] To date six *GDAP1* missense mutations with autosomal dominant inheritance pattern have been described: p.R120W, p.T157P, p.Q218E, p.C240Y, p.P274L and p.H123R.[4,7-9] Each of these mutations have been described in only one family except the p.R120W and the p.H123R changes: p.H123R has been identified in CMT patients from two unrelated families,[9] and p.R120W in six unrelated families including the present work.[4,9] The p.R120W mutation has been also described in a compound heterozygous CMT patient carrier of both p.R120W and p.G217R mutations in a heterozygous state.[26] This patient had a severe phenotype similar to the autosomal recessive *GDAP1* mutations. The p.R120W substitution was transmitted from his deceased father and unfortunately, clinical symptoms from him are not referred, therefore, he might have suffered a mild clinical picture or be an asymptomatic carrier.

GDAP1 is a mitochondrial fission protein localized in the mitochondrial outer membrane, functioning as a tail-anchored protein [27-30] that promotes fission without increasing the risk of apoptosis.[31] Little is known about how *GDAP1* mutations affect the proper function of the protein, and different malfunction in mitochondrial dynamics have been postulated according to the mode of inheritance. Recessive *GDAP1* mutations seem to lead to a reduction of fission activity whereas dominant *GDAP1* mutations may impair mitochondrial fusion and cause mitochondrial

aggregation. This latter mechanism may be similar to some pathogenic *MFN2* mutations (CMT2A) in which its mitochondrial fusion activity is not overly affected, but there is excessive mitochondrial aggregation and impairment of mitochondrial transport. [31-33] This observation emphasizes that both *GDAP1* and *MFN2* may be involved in the same pathway of axonal CMT pathophysiology, explaining the clinical and neuroimaging similarities.

ACKNOWLEDGEMENTS

We are grateful to the propositi and their relatives for their kind collaboration.

For the consecution of this project, the collaboration of other authors was necessary: Carmina Espinos, Juaj Jesús Vilchez, Dolores Martinez-Rubio, Maria Jose Chumillas, Fernando Mayordomo, Nuria, Muelas, Luis Bataller and Francesc Palau.

We also want to thank I. Llopis and M. Escutia for their help with sample management.

REFERENCES

1. Payreson D, Marchesi C. Diagnosis, natural history, and management of Charcot-Marie-Tooth disease. Lancet Neurol 2009; 8:654-667.
2. Baxter RV, Ben Othmane K, Rochelle JM, et al. Ganglioside-induced differentiation-associated protein-1 is mutant in Charcot-Marie-Tooth disease type 4A/8q21. Nature Genetics 2002; 30: 21–22.
3. Cuesta A, Pedrola L, Sevilla T, et al. The gene encoding ganglioside-induced differentiation- associated protein 1 is mutated in axonal Charcot-Marie-Tooth type 4A disease. Nature Genetics 2002; 30: 22–25.
4. Claramunt R, Pedrola L, Sevilla T, et al. Genetics of Charcot-Marie-Tooth disease type 4A: mutations, inheritance, phenotypic variability, and founder effect. J Med Genet 2005; 42: 358–365.
5. Boerkoel CF, Takashima H, Nakagawa M, et al. CMT4A: identification of a Hispanic GDAP1 founder mutation. Ann Neurol 2003; 53: 400–405.
6. Sevilla T, Cuesta A, Chumillas MJ, et al. Clinical, electrophysiological and morphological findings of Charcot-Marie-Tooth neuropathy with vocal cord palsy and mutations in the GDAP1 gene. Brain 2003;126:2023–2033
7. Chung KW, Kim SM, Sunwoo IN, et al. A novel GDAP1 Q218E mutation in autosomal dominant Charcot-Marie- Tooth disease. J Hum Genet 2008; 53:360–364
8. Cassereau J, Chevrollier A, Gueguen N al. Mitochondrial complex I deficiency in GDAP1-related autosomal dominant Charcot-Marie-Tooth disease (CMT2K). Neurogenetics 2009; 10:145-150.
9. Cavallaro T, Ferrarini M, Taioli F, et al. Autosomal dominant Charcot-Marie-Tooth disease type 2 associated with Ganglioside-induced differentiation-

associated protein 1 gene. Presented at 3rd International CMT Consortium Meeting; July 9-11, 2009; Antwerpen (Belgium).

10. Fleckenstein JL, Watumull D, Conner KE, et al. Denervated human skeletal muscle: MR imaging evaluation. Radiology 1993; 187:213–218.
11. May DA, Disler DG, Jones EA, Balkissoon AA, Manaster BJ. Abnormal signal intensity in skeletal muscle at MR imaging: patterns, pearls, and pitfalls. Radiographics 2000; 20:S295–315.
12. Shy ME, Blake J, Krajewski K, et al. Reliability and validity of the CMT neuropathy score as a measure of disability. Neurology 2005; 64:1209–1214.
13. Birouk N, Gouider R, Le Guern E, et al. Charcot–Marie–Tooth disease type 1A with 17p11.2 duplication. Clinical and electrophysiological phenotype study and factors influencing disease severity in 119 cases. Brain 1997; 120:813–823.
14. Chung KW, Suh BC, Shy ME, et. al. Different clinical and magnetic resonance imaging features between Charcot–Marie–Tooth disease type 1A and 2A. Neuromuscul Disord 2008; 18:610–618.
15. Sevilla T, Jaijo T, Nauffal D, et. al. Vocal cord paresis and diaphragmatic dysfunction are severe and frequent symptoms of *GDAP1*-associated neuropathy. Brain 2008; 131: 3051-3061.
16. Azzedine H, Ruberg M, Ente D, Gilardeau C, Périé S, Wechsler B, et al. Variability of disease progression in a family with autosomal recessive CMT associated with a S194X and new R310Q mutation in the GDAP1 gene. Neuromuscul Disord 2003; 13:341-6.
17. Moroni I, Morbin M, Milani M, et al. Novel mutations in the GDAP1 gene in patients affected with early-onset axonal Charcot-Marie-Tooth type 4A. Neuromuscul Disord 2009; 19: 476-480.

18. Senderek J, Bergmann C, Ramaekers VT, et al. Mutations in the ganglioside-induced-differentiation-associated protein-1 (GDAP1) gene in intermediate type autosomal recessive Charcot-Marie-Tooth neuropathy. Brain 2003; 126: 642-649.

19. Chung KW, Kim SB, Park KD, et al. Early onset severe and late-onset mild Charcot-Marie-Tooth disease with mitofusin 2 (MFN2) mutations. Brain 2006; 129: 2103-2118.

20. Gallardo E, Garcia A, Combarros O, Berciano J. Charcot–Marie– Tooth disease type 1A duplication: spectrum of clinical and magnetic resonance imaging features in leg and foot muscles. Brain 2006; 129:426–437.

21. Abe A, Numakura C, Saito K et al. Neurofilament light chain polypeptide gene mutations in Charcot-Marie-Tooth disease: nonsense mutation probably causes a recessive phenotype. J Hum Genet 2009; 54: 94-97.

22. Yum SW, Zhang J, Mo K, Li J, Scherer SS. A novel recessive NEFL mutation causes a severe, early-onset axonal neuropathy. Ann Neurol 2009; 66: 759-770.

23. Houlden H, Laura M, Wavrant-De Vrièze F, Blake J, Wood N, Reilly MM. Mutations in the HSP27 (HSPB1) gene cause dominant, recessive and sporadic distal HMN/CMT type 2. Neurology 2008; 71: 1660-1668.

24. Calvo J, Funalot B, Ouvrier RA et al. Genotype-Phenotype correlations in Charcot-Marie-Tooth disease type 2 caused by mitofusin 2 mutations. Arch Neurol 2009; 66: 1511-1516.

25. Nicholson GA, Magdelaine C, Zhu D, Grew S et al. Severe early-onset axonal

neuropathy with homozygous and compound heterozygous MFN2 mutations. Neurology 2008; 70: 1678-1681.

26. Ammar N, Nelis E, Merlini L, Barisić N, et al. Identification of novel GDAP mutations causing autosomal recessive Charcot-Marie-Tooth disease. Neuromuscul Disord 2003; 13:720-728.

27. Pedrola L, Espert A, Wu X, Claramunt R, Shy ME, Palau P. GDAP1, the protein causing Charcot-Marie-Tooth disease type 4A, is expressed in neurons and is associated with mitochondria. Hum Mol Genet 2005; 14:1087-1094.

28. Niemann A, Ruegg M, La Padula V, Schenone A, Suter U . Ganglioside-induced differentiation associated protein 1 is a regulator of the mitochondrial network: new implications for Charcot-Marie-Tooth disease. J Cell Biol 2005; 170:1067-1078.

29. Pedrola L, Espert A, Valdés-Sánchez T, et al. Cell expression of GDAP1 in the nervous system and pathogenesis of Charcot-Marie-Tooth type 4A disease. J Cell Mol Med 2008; 12:679-689.

30. Wagner KM, Rüegg M, Niemann A, Suter U. Targeting and function of the mitochondrial fission factor GDAP1 are dependent on its tail-anchor. PLoS ONE 2009;4:e5160

31. Niemann A, Wagner KM, Ruegg M, Suter U. GDAP1 mutations differ in their effects on mitochondrial dynamics and apoptosis depending on the mode of inheritance. Neurobiol Dis 2009; 36:509-520.

32. Detmer SA, Chan DC. Complementation between mouse Mfn1 and Mfn2 protects mitochondrial fusion defects caused by CMT2A disease mutations. J Cell Biol 2007; 176:405-414.

33. Baloh RH, Schmidt RE, Pestronk A, Milbrandt J. Altered axonal mitochondrial transport in the pathogenesis of Charcot-Marie-Tooth disease from mitofusin 2 mutations. J Neurosci 2007; 27: 422-430.

FIGURES & LEGENDS

Figure 1. Pedigrees of the 4 affected families

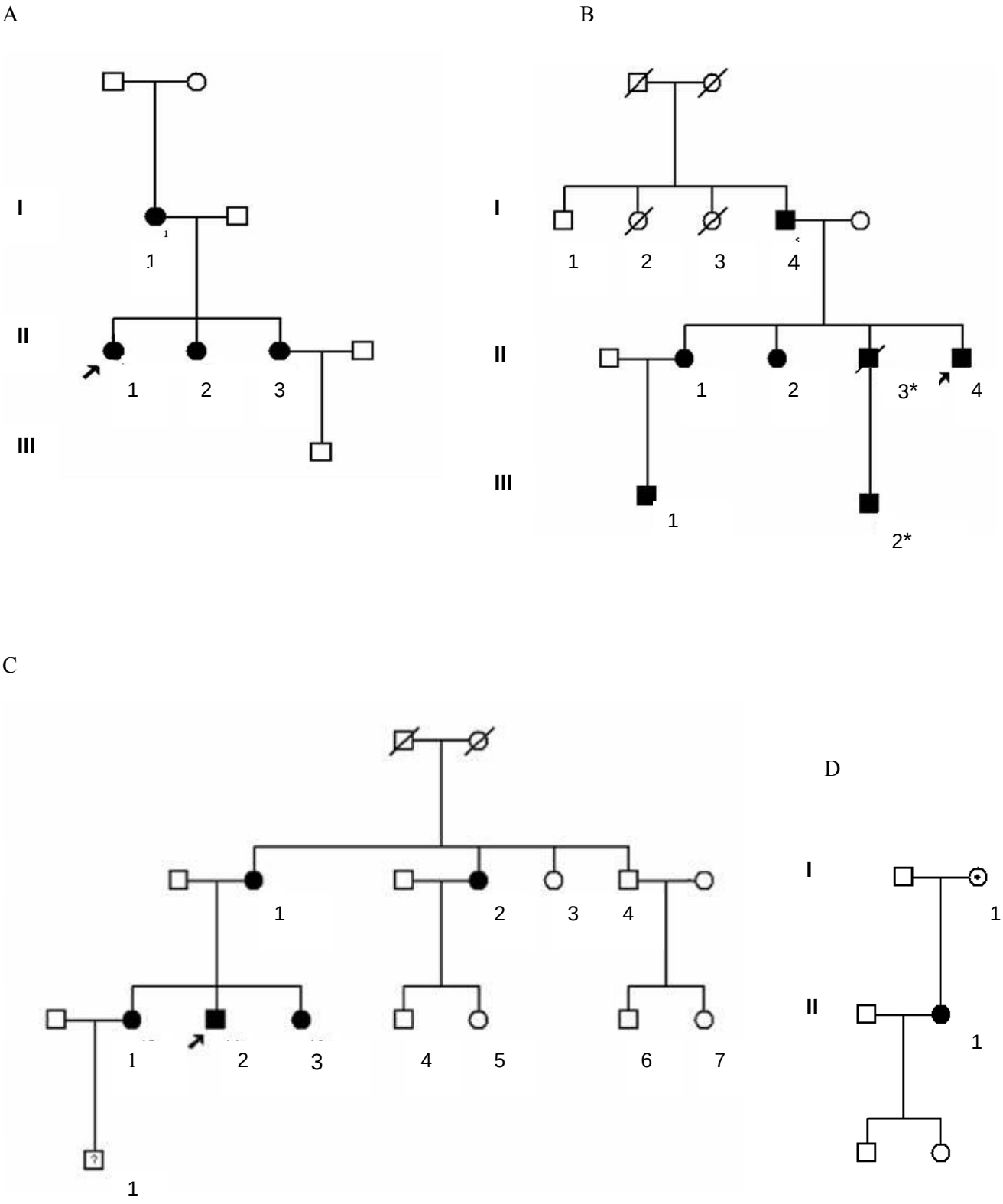

Squares = males, circles = females, shaded symbols = affected, dot = affected by history. Family B has been previously reported[4] and includes two individuals (*) who have not been clinically assessed in this moment.

Figure 2 MRI of the foot and calf muscles in mild and severe phenotypes

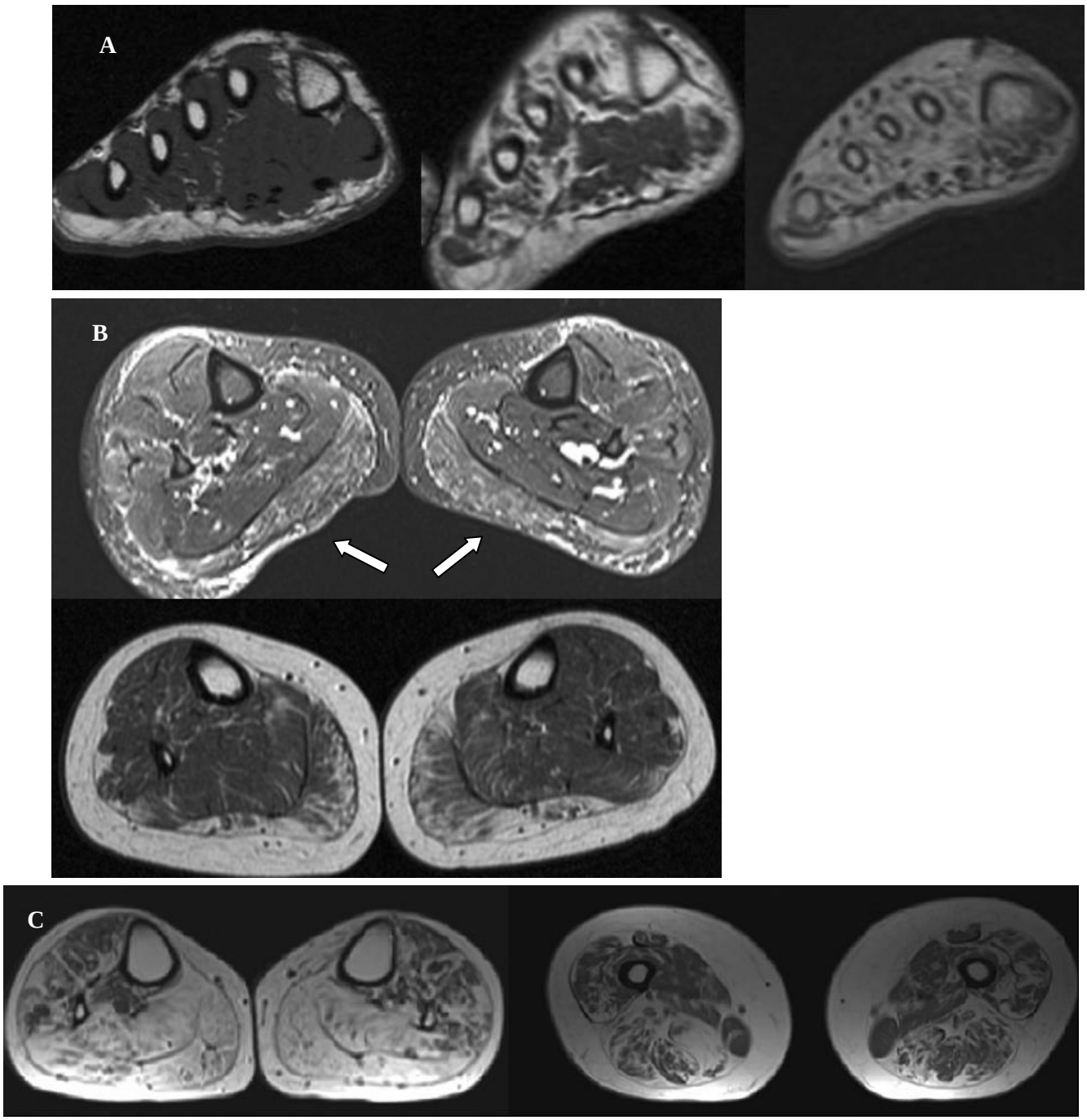

A) Axial T1 weighted images showing fatty infiltration in the intrinsic foot muscles from left to right of a control subject, an asymptomatic patient (patient A-II2) and a moderately severe patient (patient C-II2).

B) Axial STIR (above) and T1 weighted (below) images of the calf of patients with a mild phenotype (patient C-I2 & B-II1 respectively). There is muscle edema and fatty infiltration in the superficial posterior compartment of the calf (arrows).

C) Axial T1 weighted images of the calf (left) and thigh (right) of patients with a severe phenotype (patient A-I1 & D-II1 respectively) showing fatty substitution in all the muscle compartments of the calf (posterior > anterolateral) and distal thigh.

Figure 3

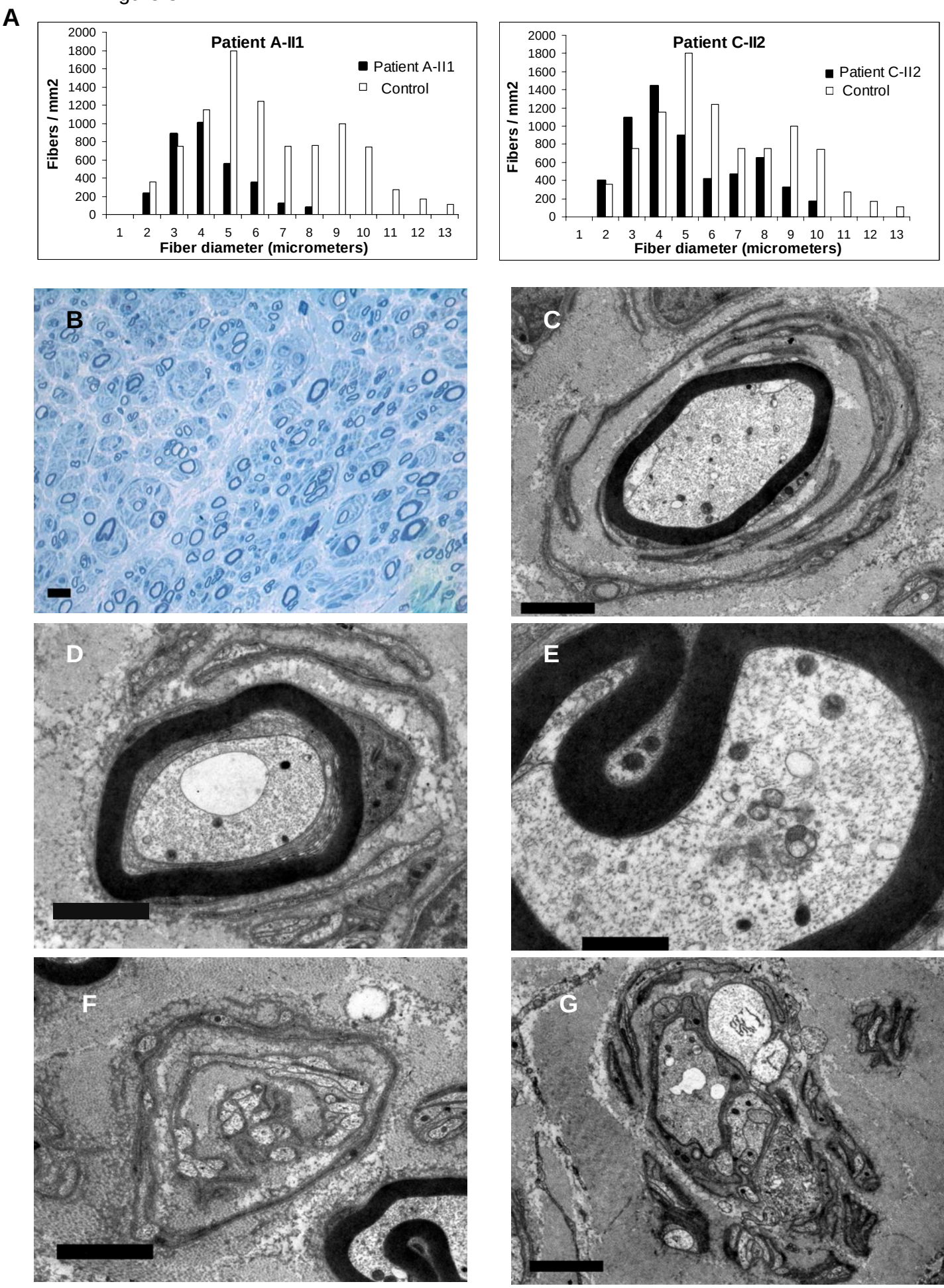
A
Patient A-II1
Patient A-II1
Control
Fibers / mm2
Fiber diameter (micrometers)
Patient C-II2
Patient C-II2
Control
Fibers / mm2
Fiber diameter (micrometers)
B
C
D
E
F
G

Figure 3.

A) Histograms representing myelinated fibre distribution of patients A-II1 and C-II2 (filled bars). Note the predominant loss of large myelianted fibres compared with a control subject (open bars).

B) Semi-thin transverse section of Patient A-II1 showing a pronounced depletion of large myelinated fibres, and myelin thickness, as well as regenerative clusters and few onion bulb formations.

Plates C to F display distinct electron microscope views. C) Onion bulb formation surrounding a thinly myelinated axon. D) Axonal atrophy with axolemma detachment from myelin sheath. E) Normally myelinated axon with focal accumulates of abnormal mitochondria and paucity of microtubules.

F) Bulb formation encircling a regenerating cluster of unmyelinated axons.

G) Regenerative cluster composed of a bundle of axons, one of them with a tiny myelin sheath, showing axoplasmic degenerative features.

Bar= 10 μm in B, 2 μm in C, D, F, G, 1 μm in E

Table 1.Clinical data of the series

Patient	Age at exam./ Onset (ys)	CMTNS	Proximal LL	Ankle DF	Ankle PF	TE	IHM	Heel/ Toe walk	UL DTR	Knee DTR	Ankle DTR	Pes cavus	Pinprick sesory loss	Vibratory sensory loss	FDS
A-I1	67/>40	21	4	2	2	0	4	I/I	+	-	-	moderate	knee/elbow	ankle	5
A-II1	43/9	14	5	3	3	0	4+	I/I	++	+	-	moderate	knee/elbow	ankle	3
A-II2	40/A	5	5	5	5	4+	5	N/D	++	++	+	mild	toes	none	0
A-II3	38/35	7	5	5	5	5	5	N/N	++	++	-	mild	ankle	toes	0
B-I4	80/65	11 *	5	2	2	2	4	I/I	-	-	-	no	ankle	ankle	4
B-II1	52/15	10	5	4	4	3	4	I/I	++	++	-	mild	ankle	none	3
B-III1	20/A	0	5	5	5	5	5	N/N	++	++	++	mild	none	none	0
B-II2	40/16	4	5	4	5	4	5	D/D	++	+	-	mild	ankle	toes	1
B-II4	38/17	12	5	4	4	3	4	D/D	++	+	-	moderate	ankle	toes	3
C-I1	62/18	9	5	5	4	3	5	D/D	++	-	-	moderate	ankle/finger	ankle	2
C-II1	33/20	6	5	5	5	5	5	D/N	++	-	-	mild	ankle	none	1
C-II2	30/14	15	5	3	$2^R/4^L$	1	4	I/I	++	-	-	moderate	ankle	ankle	2
C-II3	24/12	7	5	4	4	3	5	D/D	++	+	-	moderate	ankle	none	2
C-I2	72/A	0 *	5	5	5	5	5	N/N	++	-	-	no	none	none	0
D-II1	75/25	25	4+	0	0	0	4	I/I	-	-	-	mild	knee/finger	ankle	5

A: asymptomatic, * : Patients in which only the clinical parameters were used to calculate the CMTNS score (no electrophysiological data available), LL= lower limbs, DF= dorsiflexion, ^{R} = right, ^{L} = left, PF= plantar flexion, TE = toe extension, IHM= intrinsic hand muscles. I= impossible, D= difficulty, N= normal, UL = upper limbs, DTR = deep tendon reflexes.

Table 1.Nerve conductions and MRI data

Nerve conduction studies											MRI						
Patient	Median		Ulnar		Peroneal		Median		Sural		IFM	Soleus	Gastroc-nemius	DPC	AC	LC	Thigh
	CMAP mv	MCV m/s	CMAP mv	MCV m/s	CMAP mv	MCV m/s	SNAP μv	SCV m/s	SNAP μv	SCV m/s							
A-I1	9,4	54,8	6,1	53,5	0,6	40,3	1,6	36,3	NR	NR	-	-	-	-	-	-	-
A-II1	7,5	69	NP	NP	1,3	48	4	44	3	29	4	4	4	2	3	3	3
A-II2	9,5	60	12	60,3	5,4	42	12	57,1	1,8	50	3	2	3	0	0	1	-
A-II3	11,5	60	15,7	64,9	7,3	50,8	10	54,7	9,1	NP	2	1	1	0	0	0	-
B-II1	11,2	69,1	11,7	67,9	4	53,7	6,5	53,3	6,2	55,6	-	-	-	-	-	-	-
B-III1	17,2	61,2	20,6	69,3	11,9	45	24	50	15	65,9	-	-	-	-	-	-	-
B-II2	12,1	60,3	14,4	52,3	4	43,8	26	60	9,9	48,2	-	-	-	-	-	-	-
B-II3	9,1	59	NP	NP	1,8	47	8,5	49	0,5	41	-	-	-	-	-	-	-
B-II4	11,7	56,5	13,6	57,5	2,1	40,8	2,8	47,4	6,6	33,3	-	-	-	-	-	-	-
C-I1	NP	NP	NP	NP	7,9	42,5	NR	NR	1,1	37,6	4	3	4	0	1	1	-
C-II1	18,5	57	NP	NP	15	39	4,5	NP	0.7	-	-	-	-	-	-	-	-
C-II2	15	56,3	13,7	59,2	0,5	-	5,8	40,7	4,5	38,2	4	4	4	1	2	2	-
C-II3	8	56	NP	NP	5,2	45	1,6	-	NR	NR	4	4	4	1	1	1	-
C-I2	-	-	-	-	-	-	-	-			3	1	2	0	0	1	-
D-II1	6.6	53.8	5.6	50	NR	NR	NR	NR	0.7	37.1	4	4	4	3	4	4	3

CMAP= compound muscle action potential, MCV= motor nerve conduction velocity, SCV= sensory conduction velocity, SNAP= compound sensory nerve action potential. NP= not performed; NR= no response, IFM= intrinsic foot muscles, DPC= deep posterior compartment, AC= Anterior compartment, LC= lateral compartment.